Letter

Liouvillian skin effects and fragmented condensates in an integrable dissipative Bose-Hubbard model

Christopher Ekman [*] and Emil J. Bergholtz [†]

Department of Physics, Stockholm University, AlbaNova University Center, 10691 Stockholm, Sweden

(Received 23 February 2024; revised 4 June 2024; accepted 31 July 2024; published 17 September 2024)

Strongly interacting nonequilibrium systems are of great fundamental interest, yet their inherent complexity make them notoriously hard to analyze. We demonstrate that the dynamics of the Bose-Hubbard model, which by itself evades solvability, can be solved exactly at any interaction strength in the presence of loss tuned to a rate matching the hopping amplitude. Remarkably, the full solvability of the corresponding Liouvillian, and the integrability of the pertinent effective non-Hermitian Hamiltonian, survives the addition of disorder and generic boundary conditions. By analyzing the Bethe ansatz solutions we find that even weak interactions change the qualitative features of the system, leading to an intricate dynamical phase diagram featuring non-Hermitian Mott-skin effects, disorder induced localization, highly degenerate exceptional points, and a Bose glasslike phase of fragmented condensates. We discuss realistic implementations of this model with cold atoms.

DOI: 10.1103/PhysRevResearch.6.L032067

Introduction. In cold atom systems with strong interactions [1–5] and disorder [6], dissipation is an ever-present adversary, since environmental coupling tends to destroy intriguing, but delicate, quantum phenomena. However, it is being increasingly appreciated that dissipation itself may in fact be harnessed [7–21] and induce unique intriguing effects [19–22], thus providing a new frontier in the study of nonequilibrium quantum many-body systems [23]. The vast majority of recent studies have focused on noninteracting dissipative systems [19–21]. In the quantum realm these systems may realize novel topological phenomena such as the Liouvillian version [24–27] of the non-Hermitian skin effect [28–34] in which a macroscopic number of eigenstates are exponentially localized at the boundaries of the system. Several recent studies investigate the interplay between interactions and the skin effect [35–44], yet this topic remains far less explored than the noninteracting case.

Even in the absence of dissipation, strongly interacting models are difficult to analyze. This in particular applies to the paradigmatic one-dimensional Bose-Hubbard model [45,46], which is famously nonintegrable [47] for more than two sites [48], in contrast to its fermionic counterpart. The absence of integrability combined with its key experimental importance [49] has made it a popular target in numerical studies, using, for example, density, renormalization group techniques [50–55], Monte Carlo methods [56,57], and exact diagonalization [55,58,59].

A seminal exact solution strategy of a strongly interacting many body system was provided by Bethe [60] in his famous exact solution of the Heisenberg model. Much more recently, third quantization [61] was invented as a framework to solve quadratic (noninteracting) Liouvillians, describing driven-dissipative systems, and in the last few years the notion of integrability was extended to more general systems including certain interacting Liouvillians [62–66]. The application of integrability methods to the solution of Liouvillians has thus made it possible to construct exactly solvable models that combine both dissipation and strong interactions, but exactly solvable models of that kind are rare, and exactly solvable models that incorporate disorder, dissipation, and interactions simultaneously remain elusive.

In this Letter, we present and analytically solve a disordered Bose-Hubbard chain with environmental coupling that is tailored to render it exactly solvable while remaining realistic in cold atom systems (see Fig. 1). In the process we derive and solve the non-Hermitian Hamiltonian of the unidirectional Bose-Hubbard chain that was first shown to be Yang-Baxter integrable in Ref. [40]. Here we extend this analysis in several ways that reveal qualitatively new physics. We show how the model emerges as an effective description of a realistic setup, and that it remains integrable in the presence of arbitrary on-site potentials, including random on-site disorder, and with open boundary conditions. The open boundary conditions enable non-Hermitian Mott-skin effects and highly degenerate exceptional points, and adding disorder leads to a phase that is reminiscent of a Bose glass. Furthermore, we stress that our analysis goes beyond the effective non-Hermitian Hamiltonian approach by providing a complete solution of the Lindblad Liouvillian.

Model and physical realization. Dissipative cold atom systems may be realistically modeled using the Lindblad master

[*]Contact author: christopher.ekman@fysik.su.se
[†]Contact author: emil.bergholtz@fysik.su.se

Published by the American Physical Society under the terms of the Creative Commons Attribution 4.0 International license. Further distribution of this work must maintain attribution to the author(s) and the published article's title, journal citation, and DOI. Funded by Bibsam.

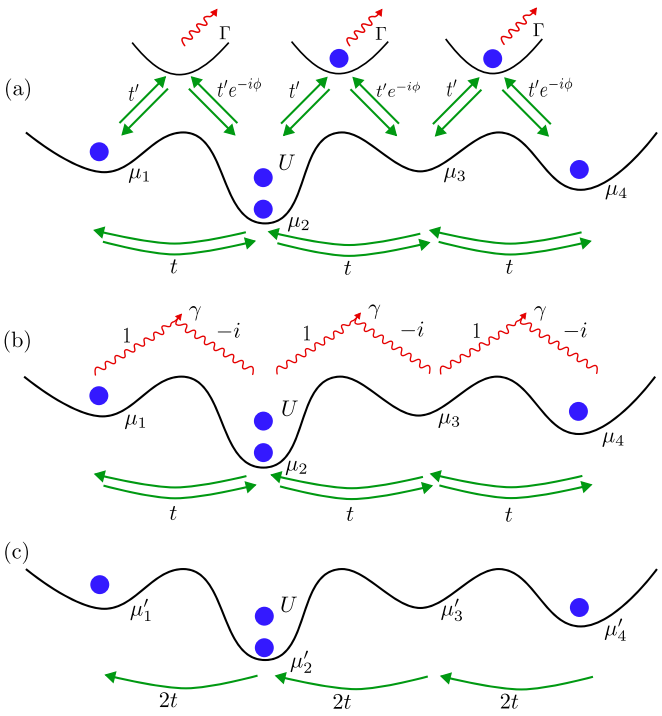


FIG. 1. The models under consideration in this Letter. (a) A triangular ladder as implemented in Refs. [13,14], with an additional on-site potential and interactions of strength U. The upper sites have dissipation with rate Γ, while the lower ones do not. A fictitious magnetic flux ϕ leads to a relative phase in the hopping terms between the different sites. Upon integrating out the green sites, we obtain (b) with dissipation acting on neighboring sites, where the magnetic flux has been chosen to be $\phi = \frac{\pi}{2}$. (c) shows the system described by the integrable unidirectional effective non-Hermitian (4), where the dissipation has been absorbed into the hopping parameter and the on-site potential.

equation [67,68],

$$\frac{d\rho}{dt} = \mathcal{L}\rho = -i[H,\rho] + \sum_j \gamma_j (2\ell_j \rho \ell_j^\dagger - \{\ell_j \ell_j^\dagger, \rho\}), \quad (1)$$

with $\gamma_j \geqslant 0$. We consider the coherent dynamics to be described by the disordered Bose-Hubbard Hamiltonian

$$H = -t\sum_{j=1}^{N} a_j^\dagger a_{j+1} + a_{j+1}^\dagger a_j + \frac{U}{2}\sum_{j=1}^{N} n_j(n_j-1) + \sum_{j=1}^{N} \mu_j n_j, \quad -\epsilon(a_N^\dagger a_1 + a_1^\dagger a_N) \quad (2)$$

where a_j are bosonic annihilation operators, $n_j = a_j^\dagger a_j$ are the number operators, and μ_j are disorder variables.

One way to incorporate realistic dissipation so that the system becomes exactly solvable is to consider a triangular ladder [13,14], as in Fig. 1(a). Particles dissipate from the sites on the top and these sites can be integrated out [69] (see also Ref. [70]), leaving a chain with jump operators

$$\ell_j = a_j - i a_{j+1}, \quad (3)$$

as in Fig. 1(b), cf. Ref. [24]. The relative phase factor may be obtained experimentally by including a magnetic field. Remarkably, at the level of the effective non-Hermitian Hamiltonian, the hopping in one direction vanishes if $\gamma_j = t$ for $j \neq N$ and $\gamma_N = \frac{\epsilon}{2}$. Explicitly, the resulting effective non-Hermitian Hamiltonian [Fig. 1(c)] becomes

$$H_{eff} = -2t\sum_{j=1}^{N} a_j^\dagger a_{j+1} + \frac{U}{2}\sum_{j=1}^{N} n_j(n_j-1) + \sum_{j=1}^{N} \mu_j' n_j - \epsilon a_1^\dagger a_N, \quad (4)$$

where we defined $\mu_j' = \mu_j - 2it$ for $j \neq 1, N$ and $\mu_1' = \mu_1 - i(t + \frac{\epsilon}{2})$, $\mu_N' = \mu_N - i(t + \frac{\epsilon}{2})$. Reference [14] realized and analyzed the noninteracting and nondisordered limit of Eq. (4) in a cold atom system. Here we include both interactions and disorder, and in addition to Eq. (4), also consider the full Liouvillian quantum dynamics as described by Eqs. (1)–(3). An immediate conclusion that can be drawn is that in the absence of interactions, a state with N particles decays at a rate of $-\mathrm{Im}(\sum_j \mu_j' n_j) \approx 2tN$.

Bethe ansatz solution. Using the machinery of the quantum inverse scattering method [71], it may be shown that the right eigenvectors of the Hamiltonian, and of all its constants of motion defined in the Supplemental Material [69], have the form given by the algebraic Bethe ansatz

$$|\{\lambda_n\}\rangle = \prod_{n=1}^{M} \mathcal{B}(\lambda_n)|\Omega\rangle \quad (5)$$

for an operator $\mathcal{B}(\lambda)$ that takes a continuous argument λ. Each application of $\mathcal{B}$ creates a quasiparticle, so the state given above has M quasiparticles. In the Fock basis the vacuum $|\Omega\rangle$ is equal to the state without any particles in it. The states given by Eq. (5) are eigenvectors of the Hamiltonian if the rapidities λ_n solve the Bethe equations, which in this case are given by

$$\prod_{k=1}^{N}(\lambda_n - \mu_k')\prod_{j\neq n}(\lambda_n - \lambda_j - U) - \epsilon\left(-\frac{2t}{U}\right)^N \prod_{j\neq n}(\lambda_j - \lambda_n - U) = 0. \quad (6)$$

In terms of the rapidities, the eigenvalue corresponding to the eigenstate (5) of the non-Hermitian effective Hamiltonian is $E(\{\lambda_n\}) = \sum_{n=1}^{M} \lambda_n$. In the case without an onsite potential, meaning $\mu_k' = 0$ for all k, and with $\epsilon \neq 0$, this was first shown in Ref. [40].

The coordinate Bethe ansatz in terms of the rapidities is [72]

$$\Psi(\{x_k\}_{k=1}^M) = \sum_{\sigma\in S_M}\prod_{j>k} f(\lambda_{\sigma_j} - \lambda_{\sigma_k}) \prod_{n=1}^{M}\prod_{j=1}^{x_n}\left(\frac{\lambda_{\sigma_n} - \mu_j}{-2t}\right), \quad (7)$$

where $f(\lambda) = 1 - \frac{U}{\lambda}$, and S_M is the set of all permutations of the integers between 1 and M. This expression matches the algebraic Bethe ansatz.

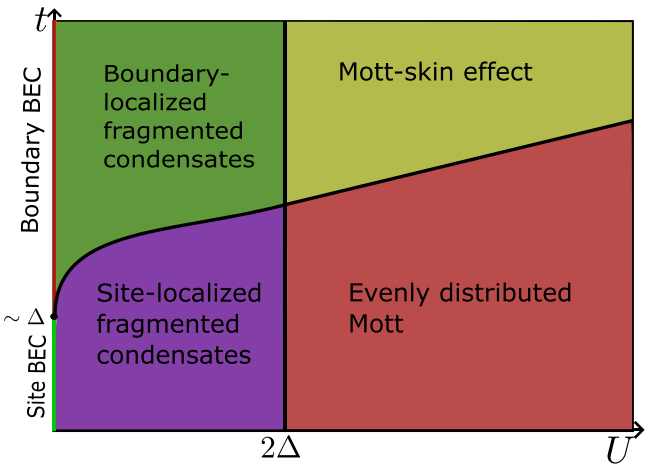


FIG. 2. The ground state phase diagram of the non-Hermitian Hamiltonian with open boundary conditions at integer filling as obtained analytically from the two-point correlation functions in Eqs. (15) and (16). For $U > 2\Delta$ the ground state is in a Mott phase, which can either be localized at the boundary or be evenly distributed depending on t, whereas for $U < 2\Delta$ the system is in Bose-glass-like phase of fragmented condensates, which may also be localized either at the boundary or at some site. At $U = 0$ there is a transition between a Bose-Einstein condensate at the boundary and a Bose-Einstein condensate at a single site in the bulk.

Integrability and solvability. The integrability structure outlined above can be used to explicitly diagonalize the Liouvillian (1). It is important that there is only dissipation (or only gain), and that the effective non-Hermitian Hamiltonian commutes with the number operator, as this ensures that the Liouvillian is triangular in the basis given by states of the form $|\{\lambda_n\}_{n=1}^{M}\rangle\langle\{\nu_m\}_{m=1}^{M'}|$ [73]. Its eigenvalues are given by

$$\omega\big(\{\lambda_n\}_{n=1}^{M},\{\nu_m\}_{m=1}^{M'}\big) = -i\sum_{n=1}^{M}\lambda_n + i\sum_{m=1}^{M'}\bar{\nu}_m, \tag{8}$$

and the eigenoperators have the form

$$\rho_{(\lambda,\nu)} = \sum_{n=0}^{m}\sum_{(\lambda',\nu')} v_{(\lambda,\nu);(\lambda',\nu')}^{(l,m;n)}|\{\lambda'\}\rangle\langle\{\nu'\}|, \tag{9}$$

where the coefficients are given in the Supplemental Material [69] (see also Refs. [74–78]). Note that the unique steady state of the system is the empty state, so there cannot be any conserved quantities. The Liouvillian therefore cannot easily be said to be integrable, in spite of the underlying integrability structure that allows its exact analytical solution.

Correlation functions and phase diagram for open boundary conditions. We now examine the properties of the model defined by the effective Hamiltonian (4) with random disorder and open boundary conditions ($\epsilon = 0$), which exhibits a remarkable degree of solvability. As we detail below this leads to the phase diagram in Fig. 2. For arbitrary disorder the Bethe equations now take the factorized form

$$\prod_{k=1}^{N}(\lambda_n - \mu_k')\prod_{j\neq n}(\lambda_n - \lambda_j - U) = 0, \tag{10}$$

which have solutions $\lambda_n^k = \mu_k' + (n-1)U$ where $n = 1, 2, \ldots$. Inserting this into the expression for the energy we see that the spectrum is given by

$$E(n_1, n_2, \ldots, n_N) = \sum_{k=1}^{N}\mu_k' n_k + \frac{U}{2}n_k(n_k - 1). \tag{11}$$

The effective Hamiltonian exhibits exceptional points, i.e., at a non-Hermitian degeneracy at which both eigenvalues and eigenstates coalesce, whenever there are distinct partitions of integers, $\{n_i\}$, giving identical energies in Eq. (11). In particular this happens when any two (or more) disorder variables, μ_i, are equal. Moreover, if the potential is constant (no disorder), there are exceptional points of very high order. It is worth noting that although at $t = 0$ the integers $\{n_i\}$ labeling energies and eigenstates correspond to particle densities, their interpretation is less straightforward at $t \neq 0$.

In the limit $U \to 0$ it is sufficient to treat the single-particle eigenstates. These are given by

$$\Psi_\lambda(x) = \prod_{j=1}^{x}\left(\frac{\lambda - \mu_j'}{-2t}\right), \tag{12}$$

which are eigenstates if $\lambda = \mu_n'$ for $n = 1, 2, \ldots, N$. If there is no disorder, meaning $\mu_n' = 0$ for all n, all the eigenstates coalesce to $\psi(x) = \delta_{x,1}$. One simple observation is in that, if $\lambda = \mu_n'$, then the particle density is zero for $x > m$ where m is the smallest integer such that $\mu_m' = \mu_n'$. The particle is therefore sharply localized to a finite region. In addition, if $t \gg |\mu_{m'}' - \mu_{n'}'|$ for all m', n' we see that the particle is exponentially localized in the left side of that region for all eigenstates. On the other hand, if $t << |\mu_{m'}' - \mu_{n'}'|$, on average each eigenstate is exponentially localized to its corresponding site. Extending to the many-body ground state, we see that it is a gapless condensate of particles in the state with λ equal to the μ_n' with smallest real part. Due to the simplicity of this state, it is possible to place strong bounds on the two-point correlation function. Let $x_2 > x_1$ both be in the region where the wave function is nonzero. Note that the imaginary parts of the μ_n:s cancel in the eigenstates, except for the factors that include μ_1' and μ_N'. These do not have a qualitative effect on the physics, so we neglect them. Using the notation $\mu_k = \mu_k' + 2it$,

$$\begin{aligned} G(x_1, x_2) &= \frac{\langle GS|a_{x_1}^\dagger a_{x_2}|GS\rangle}{\langle GS|GS\rangle} \\ &\propto \prod_{j=1}^{x_1}\left(\frac{\mu_n - \mu_j}{-2t}\right)\prod_{j=1}^{x_2}\left(\frac{\mu_n - \mu_j}{-2t}\right). \end{aligned} \tag{13}$$

In order to proceed we must place some constraints on the disorder variables. Suppose that they are bounded and not all the same. Then we may choose the smallest interval $\mathcal{I}$ such that $\mu_j \in \mathcal{I}$ for all j to be $\mathcal{I} = [-\Delta, \Delta]$ with $\Delta > 0$. Clearly, $\mu_n = -\Delta$. Suppose further that the least $\mu_m > -\Delta$ is given by $\mu_m = -\Delta + \delta$. Then the two-point correlation function satisfies the bounds

$$\frac{1}{\langle GS|GS\rangle}\left(\frac{\delta}{2t}\right)^{x_1+x_2} \leqslant |G(x_1, x_2)| \leqslant \frac{1}{\langle GS|GS\rangle}\left(\frac{\Delta}{t}\right)^{x_1+x_2} \tag{14}$$

for $x_1, x_2 < n$. If either x_1 or x_2 is greater than or equal to n then $G(x_1, x_2) = 0$. We see that the correlation length satisfies $1/\xi \in [\ln \frac{\delta}{2t}, \ln \frac{\Delta}{t}]$ and that ξ diverges for some $t \leqslant \Delta$, signifying a phase transition. One of the phases is a skin-effect phase, where all the particles are localized at one of the edges (corresponding to the red line at the left edge of Fig. 2), and the other phase is a disorder-induced localized phase, where all the particles are localized at some site (corresponding to the green line at the left edge of Fig. 2). Other states show a similar behavior.

Now we let $U > 0$. This has dramatic effects for arbitrarily weak interactions in the thermodynamic limit, $N, M \to \infty$. In the ground state the particles no longer condense into the same mode, due to the repulsive interactions. Instead, the particles spread out over the different modes, so that there are competing condensates. The Bose-Einstein condensate has fragmented due to the interactions. This is reminiscent of a Bose glass [79,80], where the competition between disorder and interactions causes disjoint localized pockets of superfluid condensate to form. Here, in contrast, the condensates are not spatially disjoint unless the disorder is much larger than the hopping parameter.

If U is sufficiently small, one of the modes will still have the largest fraction of particles, say $M_0 > M/N$ of them, so that there are rapidities $\lambda_n = -\Delta + (n-1)U$ for $n = 1, 2, \ldots, M_0$. The leading part of the two-point correlator can then be shown to satisfy

$$D\left(\frac{(M_0-1)U+\delta}{2t}\right)^X \leqslant |G(X)| \leqslant D\left(\frac{(M_0-1)U+2\Delta}{2t}\right)^X, \tag{15}$$

where we defined $X = x_1 + x_2$ and $D > 0$. We see that the correlation length satisfies $1/\xi \in [\ln \frac{(M_0-1)U+\delta}{2t}, \ln \frac{(M_0-1)U+2\Delta}{2t}]$. Clearly, ξ diverges at some point, marking a transition between a boundary-localized skin-effect phase (the purple part of Fig. 2) and a site-localized phase (the green part of Fig. 2) where M_0 particles are localized at the site where the disorder potential is minimized, while the rest are distributed in condensates elsewhere in the lattice.

If $U > 2\Delta$ the energy is minimized by equally distributing the integers in Eq. (11). Suppose for simplicity that $M/N = n$ is an integer. In that case the gap is $U - 2\Delta$, so this ground state is a Mott insulator at integer filling. The leading order behavior of the two-point correlator satisfies

$$D\left(\frac{(n-1)U+\delta}{2t}\right)^X \leqslant |G(X)| \leqslant D\left(\frac{(n-1)U+2\Delta}{2t}\right)^X \tag{16}$$

again for $D > 0$. The correlation length satisfies $1/\xi \in [\ln \frac{(n-1)U+\delta}{2t}, \ln \frac{(n-1)U+2\Delta}{2t}]$ and diverges at some point, signaling a phase transition between a boundary-localized Mott-skin effect phase and a Mott phase where the particles are evenly distributed across the lattice, as shown in the yellow and red parts of Fig. 2, respectively.

Numerical calculations corroborating these results are presented in the Supplemental Material [69].

Liouvillian dynamics. Now let us turn to the dynamics of the full Lindblad master equation. For a generic initial state we expect that the time evolution includes every eigenoperator (9), hence the two-point correlator consists of some time-dependent linear combination of all two-point correlators of the model defined by the Hamiltonian (4). By the same reasoning as for the ground state correlators, the leading order time dependent asymptotics at time τ have the form $G(X;\tau) = \sum_{n=1}^{M} D_n(\tau) g_n(X)$, where

$$\left(\frac{(n-1)U+\delta}{2t}\right)^X \leqslant |g_n(X)| \leqslant \left(\frac{(n-1)U+2\Delta}{2t}\right)^X \tag{17}$$

and the $D_n(\tau)$ are obtained from the coefficients in Eq. (9). Since there is only dissipation, it follows that the functions $D_n(\tau) \to 0$ as $\tau \to \infty$. We see that if U is nonzero there will only be a phase transition between boundary localization and site localization once the mean particle number has decreased to a finite number. If $U = 0$, on the other hand, there is always such a dynamic phase transition.

Discussion. In this work, we have shown that the paradigmatic example of a nonintegrable model, namely the Bose-Hubbard model, remarkably becomes exactly Bethe ansatz solvable in the presence of dissipation terms that may be realistically implemented with cold atoms. The effective non-Hermitian Hamiltonian as well as the full nonequilibrium quantum dynamics feature a rich phase diagram that invites ample future theoretical as well as experimental work.

As mentioned above, the realization of a momentum-space lattice version of this model in the noninteracting limit in a cold atom setup was reported in Ref. [13]. There the parameters were chosen so that interactions were unimportant and attractive. We expect that similar setups can be tuned to the regime of repulsive interactions described in this paper, although the real-space interactions must be chosen to be attractive in order to be repulsive in the momentum-space lattice [81]. While previous realizations of the noninteracting limit have used ^{87}Rb atoms, ^{39}K may be more suitable for the interacting system, as its relevant Feschbach resonances are wider, allowing for more precise control of the interactions [82]. The existing experimental implementations of the noninteracting limit can therefore be modified to include interactions, which we expect would exhibit the phase transitions described above.

The model studied in this work may be generalized to higher dimensions and more involved interaction terms. To this end one has to devise Lindblad operators such that the particles in the system can only hop in one direction along each dimension. Then the Fock basis can be ordered so that the kinetic term is triangular, and consequently the non-Hermitian effective Hamiltonian and the Liouvillian are triangular as long as the remaining terms are polynomial in the on-site densities. If open boundary conditions are chosen, it is straightforward to calculate the eigenvalues of the effective Hamiltonian, while determining the corresponding eigenvectors is technically more complicated.

An interesting conceptual aspect of this work is that the Lindbladian does not have any conserved quantities, yet it is solvable by the Bethe ansatz, similarly to the models

discussed in [65,66]. There, however, the system is integrable in the absence of dissipation in contrast to the present case [47].

The topological nature of the noninteracting non-Hermitian skin effect suggests that the quantum many-body generalizations thereof studied here is also robust to generic perturbations, which is promising in the context of its realization.

Finally, we also note that an alternative interpretation of the non-Hermitian Hamiltonian Eq. (4) can be gleaned from [83–85]. There the difference in the hopping to the left and to the right, respectively, are obtained from the strength of a magnetic field applied to interacting flux lines in an array of defects in a superconductor. The unidirectional Hamiltonian is obtained when the transverse field component is large.

Acknowledgments. We acknowledge helpful discussions with R. Arouca and A. Fagerlund. This work was supported by the Swedish Research Council (VR, Grant No. 2018-00313), the Wallenberg Academy Fellows program of the Knut and Alice Wallenberg Foundation (2018.0460), and the Göran Gustafsson Foundation for Research in Natural Sciences and Medicine.

[1] I. Bloch, J. Dalibard, and W. Zwerger, Many-body physics with ultracold gases, Rev. Mod. Phys. **80**, 885 (2008).

[2] T. Kinoshita, T. Wenger, and D. Weiss, A quantum Newton's cradle, Nature (London) **440**, 900 (2006).

[3] M. Lewenstein, A. Sanpera, V. Ahufinger, B. Damski, A. Sen(De), and U. Sen, Ultracold atomic gases in optical lattices: mimicking condensed matter physics and beyond, Adv. Phys. **56**, 243 (2007).

[4] C. Gross and I. Bloch, Quantum simulations with ultracold atoms in optical lattices, Science **357**, 995 (2017).

[5] D.-W. Zhang, Y.-Q. Zhu, Y. X. Zhao, H. Yan, and S.-L. Zhu, Topological quantum matter with cold atoms, Adv. Phys. **67**, 253 (2018).

[6] J.-C. Garreau, Quantum simulation of disordered systems with cold atoms, C. R. Phys. **18**, 31 (2017), prizes of the French Academy of Sciences 2015 / Prix de l'Académie des sciences 2015.

[7] S. Diehl, A. Micheli, A. Kantian, B. Kraus, H. Büchler, and P. Zoller, Quantum states and phases in driven open quantum systems with cold atoms, Nat. Phys. **4**, 878 (2008).

[8] C.-E. Bardyn, M. A. Baranov, C. V. Kraus, E. Rico, A. İmamoğlu, P. Zoller, and S. Diehl, Topology by dissipation, New J. Phys. **15**, 085001 (2013).

[9] N. Goldman, J. C. Budich, and P. Zoller, Topological quantum matter with ultracold gases in optical lattices, Nat. Phys. **12**, 639 (2016).

[10] M. Müller, S. Diehl, G. Pupillo, and P. Zoller, Engineered open systems and quantum simulations with atoms and ions, Adv. At. Mol. Opt. Phy., **61**, 1 (2012).

[11] S. Helmrich, A. Arias, G. Lochead, T. M. Wintermantel, M. Buchhold, S. Diehl, and S. Whitlock, Signatures of self-organized criticality in an ultracold atomic gas, Nature (London) **577**, 481 (2020).

[12] K. Sponselee, L. Freystatzky, B. Abeln, M. Diem, B. Hundt, A. Kochanke, T. Ponath, B. Santra, L. Mathey, K. Sengstock, and C. Becker, Dynamics of ultracold quantum gases in the dissipative fermi-hubbard model, Quantum Sci. Technol. **4**, 014002 (2018).

[13] W. Gou, T. Chen, D. Xie, T. Xiao, T.-S. Deng, B. Gadway, W. Yi, and B. Yan, Tunable nonreciprocal quantum transport through a dissipative Aharonov-Bohm ring in ultracold atoms, Phys. Rev. Lett. **124**, 070402 (2020).

[14] Q. Liang, D. Xie, Z. Dong, H. Li, H. Li, B. Gadway, W. Yi, and B. Yan, Dynamic signatures of non-Hermitian skin effect and topology in ultracold atoms, Phys. Rev. Lett. **129**, 070401 (2022).

[15] I. Bouchoule, L. Dubois, and L.-P. Barbier, Losses in interacting quantum gases: Ultraviolet divergence and its regularization, Phys. Rev. A **104**, L031304 (2021).

[16] K. Yamamoto and N. Kawakami, Universal description of dissipative Tomonaga-Luttinger liquids with SU(n) spin symmetry: Exact spectrum and critical exponents, Phys. Rev. B **107**, 045110 (2023).

[17] S. S. Hegde, T. Ehmcke, and T. Meng, Edge-selective extremal damping from topological heritage of dissipative Chern insulators, Phys. Rev. Lett. **131**, 256601 (2023).

[18] F. Yang, P. Molignini, and E. J. Bergholtz, Dissipative boundary state preparation, Phys. Rev. Res. **5**, 043229 (2023).

[19] Z. Gong, Y. Ashida, K. Kawabata, K. Takasan, S. Higashikawa, and M. Ueda, Topological phases of non-Hermitian systems, Phys. Rev. X **8**, 031079 (2018).

[20] Y. Ashida, Z. Gong, and M. Ueda, Non-Hermitian physics, Adv. Phys. **69**, 249 (2020).

[21] E. J. Bergholtz, J. C. Budich, and F. K. Kunst, Exceptional topology of non-Hermitian systems, Rev. Mod. Phys. **93**, 015005 (2021).

[22] D. S. Grün, K. Wittmann W, L. H. Ymai, J. Links, and A. Foerster, Protocol designs for noon states, Commun. Phys. **5**, 36 (2022).

[23] J. Eisert, M. Friesdorf, and C. Gogolin, Quantum many-body systems out of equilibrium, Nat. Phys. **11**, 124 (2015).

[24] F. Song, S. Yao, and Z. Wang, Non-Hermitian skin effect and chiral damping in open quantum systems, Phys. Rev. Lett. **123**, 170401 (2019).

[25] T. Haga, M. Nakagawa, R. Hamazaki, and M. Ueda, Liouvillian skin effect: Slowing down of relaxation processes without gap closing, Phys. Rev. Lett. **127**, 070402 (2021).

[26] F. Yang, Q.-D. Jiang, and E. J. Bergholtz, Liouvillian skin effect in an exactly solvable model, Phys. Rev. Res. **4**, 023160 (2022).

[27] L. Mao, X. Yang, M.-J. Tao, H. Hu, and L. Pan, Liouvillian skin effect in a one-dimensional open many-body quantum system with generalized boundary conditions, arXiv:2401.15614.

[28] T. E. Lee, Anomalous edge state in a non-Hermitian lattice, Phys. Rev. Lett. **116**, 133903 (2016).

[29] S. Yao and Z. Wang, Edge states and topological invariants of non-Hermitian systems, Phys. Rev. Lett. **121**, 086803 (2018).

[30] F. K. Kunst, E. Edvardsson, J. C. Budich, and E. J. Bergholtz, Biorthogonal bulk-boundary correspondence in non-Hermitian systems, Phys. Rev. Lett. **121**, 026808 (2018).
[31] V. M. Martinez Alvarez, J. E. Barrios Vargas, and L. E. F. Foa Torres, Non-Hermitian robust edge states in one dimension: Anomalous localization and eigenspace condensation at exceptional points, Phys. Rev. B **97**, 121401 (2018).
[32] N. Okuma, K. Kawabata, K. Shiozaki, and M. Sato, Topological origin of non-Hermitian skin effects, Phys. Rev. Lett. **124**, 086801 (2020).
[33] N. Okuma and M. Sato, Non-Hermitian topological phenomena: A review, Annu. Rev. Condens. Matter Phys. **14**, 83 (2023).
[34] R. Lin, T. Tai, L. Li, and C. H. Lee, Topological non-Hermitian skin effect, Front. Phys. **18**, 53605 (2023).
[35] T. Yoshida, S.-B. Zhang, T. Neupert, and N. Kawakami, Non-Hermitian Mott skin effect, Phys. Rev. Lett. **133**, 076502 (2024).
[36] B. H. Kim, J.-H. Han, and M. J. Park, Collective non-Hermitian skin effect: Point-gap topology and the doublon-holon excitations in non-reciprocal many-body systems, Commun. Phys. **7**, 73 (2024).
[37] K. Yang, S. C. Morampudi, and E. J. Bergholtz, Exceptional spin liquids from couplings to the environment, Phys. Rev. Lett. **126**, 077201 (2021).
[38] L. Mao, Y. Hao, and L. Pan, Non-Hermitian skin effect in a one-dimensional interacting Bose gas, Phys. Rev. A **107**, 043315 (2023).
[39] H.-R. Wang, B. Li, F. Song, and Z. Wang, Scale-free non-Hermitian skin effect in a boundary-dissipated spin chain, Scipost Phys. **15**, 191 (2023).
[40] M. Zheng, Y. Qiao, Y. Wang, J. Cao, and S. Chen, Exact solution of the Bose-Hubbard model with unidirectional hopping, Phys. Rev. Lett. **132**, 086502 (2024).
[41] F. Alsallom, L. Herviou, O. V. Yazyev, and M. Brzezińska, Fate of the non-Hermitian skin effect in many-body fermionic systems, Phys. Rev. Res. **4**, 033122 (2022).
[42] R. Shen and C. H. Lee, Non-Hermitian skin clusters from strong interactions, Commun. Phys. **5**, 238 (2022).
[43] S. Hamanaka and K. Kawabata, Multifractality of many-body non-Hermitian skin effect, arXiv:2401.08304.
[44] P. Zhong, W. Pan, H. Lin, X. Wang, and S. Hu, Density-matrix renormalization group algorithm for non-Hermitian systems, arXiv:2401.15000.
[45] H. A. Gersch and G. C. Knollman, Quantum cell model for bosons, Phys. Rev. **129**, 959 (1963).
[46] D. Jaksch and P. Zoller, The cold atom Hubbard toolbox, Ann. Phys. **315**, 52 (2005), special issue.
[47] T. C. Choy and F. D. M. Haldane, Failure of Bethe-Ansatz solutions of generalisations of the Hubbard chain to arbitrary permutation symmetry, Phys. Lett. A **90**, 83 (1982).
[48] J. Links, H.-Q. Zhou, R. H. McKenzie, and M. D. Gould, Algebraic Bethe Ansatz method for the exact calculation of energy spectra and form factors: applications to models of Bose–Einstein condensates and metallic nanograins, J. Phys. A: Math. Gen. **36**, R63 (2003).
[49] D. Jaksch, C. Bruder, J. I. Cirac, C. W. Gardiner, and P. Zoller, Cold bosonic atoms in optical lattices, Phys. Rev. Lett. **81**, 3108 (1998).
[50] C. Kollath, U. Schollwöck, J. von Delft, and W. Zwerger, Spatial correlations of trapped one-dimensional bosons in an optical lattice, Phys. Rev. A **69**, 031601(R) (2004).
[51] T. D. Kühner and H. Monien, Phases of the one-dimensional Bose-Hubbard model, Phys. Rev. B **58**, R14741(R) (1998).
[52] S. Ejima, H. Fehske, and F. Gebhard, Dynamic properties of the one-dimensional Bose-Hubbard model, Europhys. Lett. **93**, 30002 (2011).
[53] L. Urba, E. Lundh, and A. Rosengren, One-dimensional extended Bose-Hubbard model with a confining potential: a DMRG analysis, J. Phys. B: At., Mol. Opt. Phys. **39**, 5187 (2006).
[54] B. Schmidt and M. Fleischhauer, Exact numerical simulations of a one-dimensional trapped Bose gas, Phys. Rev. A **75**, 021601(R) (2007).
[55] C. Kollath, A. M. Läuchli, and E. Altman, Quench dynamics and nonequilibrium phase diagram of the Bose-Hubbard model, Phys. Rev. Lett. **98**, 180601 (2007).
[56] V. A. Kashurnikov, A. V. Kravasin, and B. V. Svistunov, Mott-insulator-superfluid-liquid transition in a one-dimensional bosonic Hubbard model: Quantum Monte Carlo method, JETP Lett. **64**, 99 (1996).
[57] L. Pollet, A review of Monte Carlo simulations for the Bose–Hubbard model with diagonal disorder, C. R. Phys. **14**, 712 (2013).
[58] T. Sowiński, Exact diagonalization of the one-dimensional Bose-Hubbard model with local three-body interactions, Phys. Rev. A **85**, 065601 (2012).
[59] J. M. Zhang and R. X. Dong, Exact diagonalization: the Bose–Hubbard model as an example, Eur. J. Phys. **31**, 591 (2010).
[60] H. Bethe, Zur theorie der metalle, Z. Phys. **71**, 205 (1931).
[61] T. Prosen, Third quantization: a general method to solve master equations for quadratic open Fermi systems, New J. Phys. **10**, 043026 (2008).
[62] M. V. Medvedyeva, F. H. L. Essler, and T. Prosen, Exact bethe Ansatz spectrum of a tight-binding chain with dephasing noise, Phys. Rev. Lett. **117**, 137202 (2016).
[63] M. de Leeuw, C. Paletta, and B. Pozsgay, Constructing integrable Lindblad superoperators, Phys. Rev. Lett. **126**, 240403 (2021).
[64] A. A. Ziolkowska and F. Essler, Yang-Baxter integrable Lindblad equations, SciPost Physics **8**, 044 (2020).
[65] B. Buča, C. Booker, M. Medenjak, and D. Jaksch, Bethe ansatz approach for dissipation: exact solutions of quantum many-body dynamics under loss, New J. Phys. **22**, 123040 (2020).
[66] M. Nakagawa, N. Kawakami, and M. Ueda, Exact Liouvillian spectrum of a one-dimensional dissipative Hubbard model, Phys. Rev. Lett. **126**, 110404 (2021).
[67] G. Lindblad, On the generators of quantum dynamical semigroups, Commun. Math. Phys. **48**, 119 (1976).
[68] H.-P. Breuer and F. Petruccione, *The Quantum Theory of Open Quantum Systems* (Oxford University Press, 2002).
[69] See Supplemental Material at http://link.aps.org/supplemental/10.1103/PhysRevResearch.6.L032067 for details, including Section 1 derivation of the effective Lindbladian; Section 2

details on the algebraic Bethe Ansatz; Section 3 diagonalizing the Liouvillian; and Section 4 the particle densities numerical results.

[70] A. Kamenev, *Field Theory of Non-Equilibrium Systems* (Cambridge University Press, 2023).

[71] V. E. Korepin, A. G. Izergin, and N. M. Bogoliubov, *Quantum Inverse Scattering Method and Correlation Functions* (Cambridge University Press, 2010).

[72] Y. Jiang and B. Pozsgay, On exact overlaps in integrable spin chains, J. High Energy Phys. 06 (2020) 045110.

[73] J. M. Torres, Closed-form solution of Lindblad master equations without gain, Phys. Rev. A **89**, 052133 (2014).

[74] N. Slavnov, Calculation of scalar products of wave functions and form factors in the framework of the alcebraic Bethe Ansatz, Theor. Math. Phys. **79**, 502 (1989).

[75] V. Gaudin, *La Fonction D'onde De Bethe* (Masson, 1983).

[76] T. Oota, Quantum projectors and local operators in lattice integrable models, J. Phys. A: Math. Gen. **37**, 441 (2004).

[77] D. C. Brody, Biorthogonal quantum mechanics, J. Phys. A: Math. Theor. **47**, 035305 (2014).

[78] N. Slavnov, *Algebraic Bethe Ansatz and Correlation Functions* (World Scientific, 2022).

[79] M. P. A. Fisher, P. B. Weichman, G. Grinstein, and D. S. Fisher, Boson localization and the superfluid-insulator transition, Phys. Rev. B **40**, 546 (1989).

[80] R. T. Scalettar, G. G. Batrouni, and G. T. Zimanyi, Localization in interacting, disordered, Bose systems, Phys. Rev. Lett. **66**, 3144 (1991).

[81] F. A. An, E. J. Meier, J. Ang'ong'a, and B. Gadway, Correlated dynamics in a synthetic lattice of momentum states, Phys. Rev. Lett. **120**, 040407 (2018).

[82] J. Meier, Momentum-Space Lattices for Ultracold Atoms, Ph.D. thesis, University of Illinois at Urbana-Champaign, 2019.

[83] N. Hatano and D. R. Nelson, Localization transitions in non-Hermitian quantum mechanics, Phys. Rev. Lett. **77**, 570 (1996).

[84] N. Hatano and D. R. Nelson, Vortex pinning and non-Hermitian quantum mechanics, Phys. Rev. B **56**, 8651 (1997).

[85] R. A. Lehrer and D. R. Nelson, Vortex pinning and the non-Hermitian Mott transition, Phys. Rev. B **58**, 12385 (1998).